Article

Health indicator evaluation for condition monitoring of industrial robot gears

Corbinian Nentwich [1,†] 0000-0001-8845-9999, **Gunther Reinhart** [2,*]

[1] corbinian.nentwich@iwb.tum.de
[2] emeritus.reinhart@tum.de
* Correspondence: corbinian.nentwich@iwb.tum.de
† Current address: Boltzmannstraße 15, 85747 Garching

Abstract: Condition monitoring of industrial robots has the potential to decrease downtimes in highly automated production systems. We suggest a new health indicator based on vibration data measurements and compare its performance with state-of-the-art health indicators regarding different criteria. This evaluation is based on different data sets from robot test rigs. We find that the proposed health indicator can detect several faults, has low temperature sensitivity and works in instationary velocity regimes. A discussion of the validity of the results concludes our contribution.

Keywords: industrial robot, condition monitoring, health indicator

1. Introduction

Industrial robots are a fundamental part of highly automated production systems, which can be found in the automotive or electronics industry [1]. Since they operate in complex production cells and as a part of linear production lines, robot malfunctions lead to long downtimes for repair or replacement and hence to increased costs. In particular, robot gear faults are responsible for the longest downtimes because they often require the replacement of the whole robot [2]. The condition monitoring (CM) of these gears offers the potential to resolve this issue. CM is the monitoring of an asset's health using sensor data. The health state represents a wear reserve before a failure occurs. This health state is quantified with a health indicator (HI). A significant monitored change in this health indicator can be used as a decision-making aid in the planning of maintenance actions [3]. In recent years, different HIs based on vibration data for several industrial robot components such as bearings, gears and motors and their specific faults have been investigated.

[4] developed a fault detection method, which first uses a novel phase-based, time-domain averaging method to remove the deterministic part of the vibration signal. Subsequently, the root mean square and power spectrum entropy of the remaining residual signal are calculated as health indicators. [5] developed a vibration signal based CM system for SCARA robots, which in the first step uses statistical HIs of the time domain signal to detect the occurrence of a defect and in the second step uses an artificial neural network to diagnose the fault type. [6] proposed a three-layer architecture for remote fault diagnosis of industrial robot gearboxes using vibration signals. In the diagnosis layer, the authors present a performance evaluation approach using a support vector machine, a remaining useful life prediction by a Markov model and a fault type diagnosis based on a Bayesian network. The degenerative behaviour of an industrial robot gear was observed with vibration sensors by [7] as well as [8] in accelerated wear tests. After pre-processing the signals using order tracking and spectral auto-correlation, the characteristic fault frequencies were calculated and monitored by root mean square analysis, which revealed a trend correlating with increasing wear. Besides the installation

Preprints (www.preprints.org) | NOT PEER-REVIEWED | Posted: 30 April 2021 doi:10.20944/preprints202104.0797.v1

of accelerometers, other additional data sources were investigated in this context. [9] used acoustic emission technology to detect robot gearbox faults based on the ball spinning and ball passing frequency of the bearings. [10] investigated the changes of the RMS-HI and characteristic frequencies for functional and broken strain gears of industrial robots.

However, none of these publications assesses vibration data based HIs' ability to detect faults in an industry-like industrial robot application setting. It is characterized by changing robot axes' velocities, changing temperatures of the gears due to unbalanced robot utilization and unknown robot gear fault types. This is why we present a new HI for robot gear condition monitoring, which potentially copes with these characteristics. We benchmark the newly designed HI with different state-of-the-art HIs regarding the different formulated characteristics above to assess the newly designed HI's performance for CM.

2. Materials and Methods

This section is divided in two parts. First, the newly developed HI is presented. Afterwards, the methodology to evaluate the HI's performance and data sets used in this context are explained.

2.1. Time frequency based Z-score

The concept of the newly designed HI is based on two cornerstones. To deal with instationary velocity regimes, which are found in robot applications due to the typical movement patterns of a robot, the HI is based on time-frequency-domain data. Simultaneously, the HI must take into account a certain variance of this data due to environmental changes such as temperature fluctuations. This is realized by the concept of Z-scores, a common similarity measure from statistics [11]. In detail, the new HI is based on high frequency sampled acceleration sensor data. Data from one measurement is transformed to a time-frequency-spectrogram by usage of the Short-Time-Fourier-transformation, which is calculated according to Formula 1. Here, τ and ω are time and frequency indices, $x(n)$ is the time series signal of the vibration signal at timestep n and w is a windowing function with the length R.

$$spec(\tau, \omega) = |\sum_{n=-\infty}^{\infty} x(n)w(n - \tau R)e^{-j\omega n}| \tag{1}$$

To set up the HI, a certain number of vibration signal spectrograms must be collected for the robot to capture its signal signature in a healthy state with its stochastic variations. This takes place in an initialisation phase. For this, initially, two measurements must be collected. In this context, a measurement is defined as the collection of vibration data over one single movement. Based on this data, the two spectrograms are calculated. To determine whether this reference quantity of two spectrograms captures the stochastic variation of the signal, the overall mean (Formula 2) and standard deviation (Formula 3) of the spectrograms are calculated.

$$spec(\tau, \omega)_{avg} = \frac{1}{k}\sum_{i=0}^{k} spec(\tau, \omega)_i \tag{2}$$

$$std_{spec,\ overall} = \frac{1}{0,5FT}\sum_{\tau=0}^{T}\sum_{\omega=0}^{0,5F}\sqrt{\frac{\sum_{i=0}^{k}(spec(\tau, \omega)_i - spec(\tau, \omega)_{avg})^2}{k}} \tag{3}$$

In these formulas, k describes the number of measurements in the reference quantity. T is the time length of each measurement, F is the sampling frequency and $spec(\tau, \omega)_{avg}$ is the average value of $spec(\tau, \omega)$ over measurements 0 to k. Afterwards, one measurement is added to the reference quantity at a time, and again $avg_{spec,overall}$ and $std_{spec,overall}$ are calculated. Plotting these standard deviations over the number of measurements

Preprints (www.preprints.org) | NOT PEER-REVIEWED | Posted: 30 April 2021 doi:10.20944/preprints202104.0797.v1

in the reference quantity usually first shows an increase in $std_{spec,overall}$ and then a saturation as can be seen in Figure 1. If this saturation is reached, the reference quantity can sufficiently represent the stochastic behaviour of the signal signature. In the shown example this saturation is reached after 5 measurements.

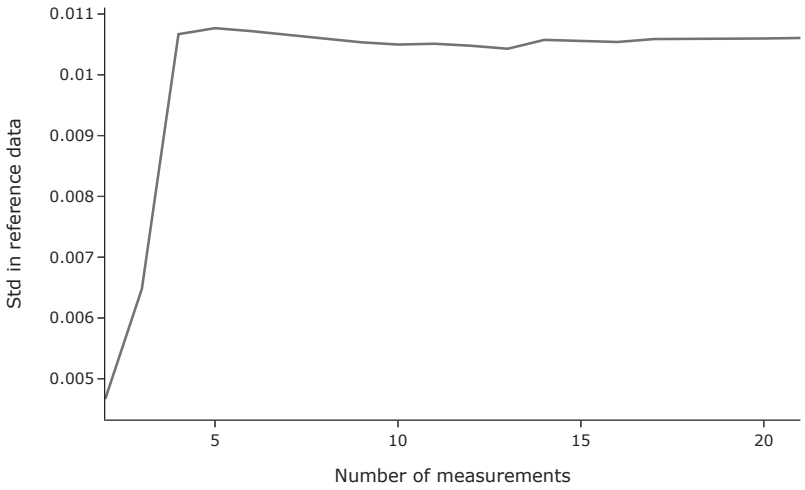

Figure 1. Saturation of the standard deviation in the time-freqency-spectrograms

After the initialisation, a HI can be determined based on a newly collected measurement. For this, the measurement's spectrogram overall Z-score is determined according to Formula 17.

$$HI_{meas} = \frac{1}{0,5FT} \sum_{\tau=0}^{T} \sum_{\omega=0}^{0,5F} \left| \frac{spec(\tau,\omega)_{meas} - spec(\tau,\omega)_{avg,ref}}{spec(\tau,\omega)_{std,ref}} \right| \tag{4}$$

In this context $spec(\tau,\omega)_{avg,ref}$ and $spec(\tau,\omega)_{std,ref}$ are the mean value and the standard deviation of $spec(\tau,\omega)$ for all measurements in the reference quantity.

2.2. HI evaluation method

To compare the ability of the newly designed HI to cope with industrial robot application characteristics, we followed a three step approach. First of all, we investigated how well the designed HI can detect different kind of faults in comparison to HIs from the state-of-the-art. Second, we investigated the temperature sensitivity of HIs from the state-of-the-art meeting this criterion and our HI. Third, we investigated the trend behaviour of HIs showing a low temperature sensitivity on data from two accelerated wear tests. These three steps are now described more precisely.

We used the FEMTO data set, which is described in detail in [12] to select HIs capable of detecting different faults. This data set provides run to failure vibration data from 16 identical bearings and for different faults and working conditions defined by the applied load and the rotational speed. The acceleration sensor sampled data with 25.6 kHz, one measurement has a length of 0.1s and measurements were taken in equidistant timesteps of 10s for all bearings. The test run for one bearing ended when the signal from the acceleration sensor exceeded 20g. We calculated the HIs summarized in Table 1 for all measurements of each sensor. These HIs were derived from several review papers regarding gearbox and bearing CM [13–16] and the publications mentioned in section 1. Therefore, the HI calculation was based either on the raw acceleration

Preprints (www.preprints.org) | NOT PEER-REVIEWED | Posted: 30 April 2021 doi:10.20944/preprints202104.0797.v1

signal, an enveloped signal as described in [17] or the residual signal as suggested by [4]. Additionally, the newly designed HI presented in section 2 was calculated for the measurements based on the raw signals.

Table 1. Calculated HIs

HI name	HI abbreviation	HI source
Crest Factor	CrF	[16]
Dominant Frequency	DomF	[13]
Impulse Factor	ImpF	[14]
Kurtosis	Kurt	[15]
Margin Factor	MarF	[14]
Mean	Mean	[16]
Median	Med	[16]
Median Frequency	MedF	[13]
Peak	Peak	[15]
Peak to Peak	PtP	[15]
Root Mean Square	RMS	[15]
Skewness	Skew	[16]
Spectral Centroid	SpC	[13]
Spectral Flux	SpF	[13]
Spectral Rollover	SpRO	[13]
Spectral Entropy	SpE	[4]
Standard Deviation	Std	[15]
Z-score	Z-score	-

To detect whether these HIs develop trends we fitted different basic functions on the HIs calculated for the last 20 percent of measurements per bearing. These functions were first and second degree polynoms, exponential and sigmoid functions. For each of the fits, we calculated the R^2 value. This means that we received four R^2 values per HI and bearing. To evaluate whether a HI can detect several damages, we considered only the best R^2 value per HI and bearing. We plotted the statistics of these 16 remaining R^2 values per HI as a boxplot. Suitable HIs should show high R^2 values with low variance.

HIs showing this behaviour were analysed regarding their temperature sensitivity. For this purpose, we acquired vibration data from an industrial robot test rig. This test rig consists of an KUKA KR510 industrial robot with an attached load of 365 kg. We attached acceleration sensors close to the gearboxes as shown in Figure 2 . These sensors have a sampling rate of 26 kHz. The acceleration dircetion of the sensors was orthogonal to their contact area. For data acquisition, the robot performed a trajectory where each joint was moved individually at different speeds in an angle area of 10° as described in Figure 3 and for different gear temperatures in the range of 25° Celsius and 60° Celsius and 5° Celsius steps. The gear temperature was measured at the gearbox cap with an infrared thermometer. For each temperature step, four measurements were made. For each measurement at each temperature step, the remaining HIs were calculated. To determine the temperature sensitivity, we divided the average HI values calculated from measurements at the highest gear temperatures by the values calculated from measurements at the lowest temperature. HIs with a high sensitivity were eliminated for the last step.

Here, we calculated the remaining HIs for measurements from two data sets from accelerated robot wear tests to see how these HIs perform in a more industry like setting and how they cope with instationary velocity behaviour. The first data set was collected during a time range of approx. one year with an ABB robot of type RB 6600-255/2.55. During the data acquisition, the robot performed an isolated movement of the second axis in an angle area of 150° for each measurement. Vibration data was only acquired with a sensor attached axially at the robot axis 2 gearbox. In the end of the experiment,

Preprints (www.preprints.org) | NOT PEER-REVIEWED | Posted: 30 April 2021 doi:10.20944/preprints202104.0797.v1

the gearbox was dismantled and faults on the bearings and the shafts of the gear were found. A total of 2290 measurements, equally distributed over time, were taken for our analysis from this data set. One measurement lasted 1.6s and the sampling rate was 10 kHz. More detailed information about this experiment can be found in [7,8].

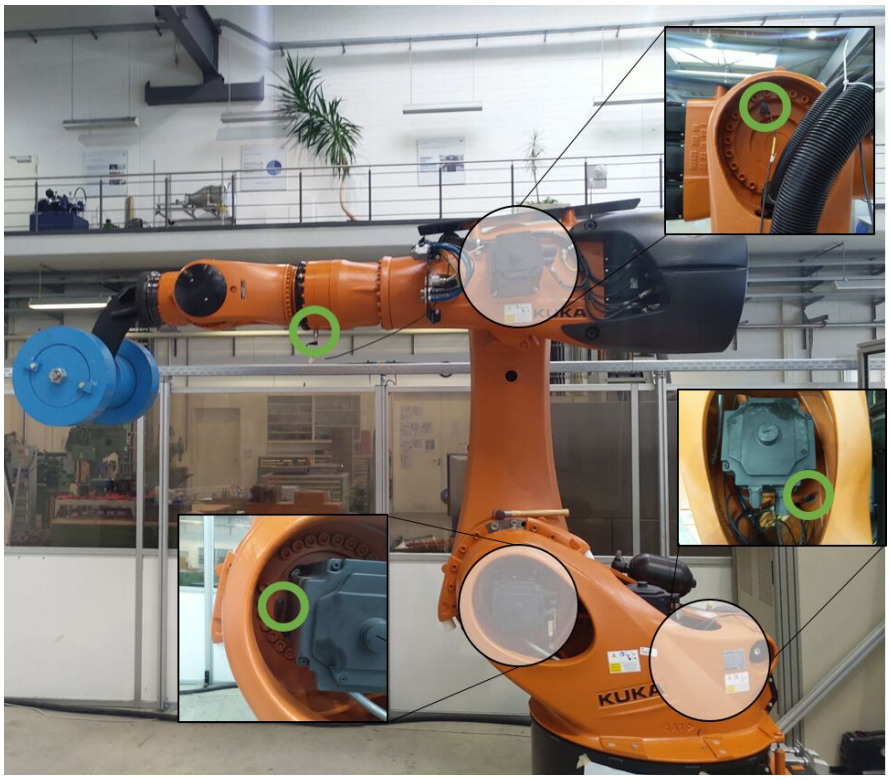

Figure 2. Robot test rig

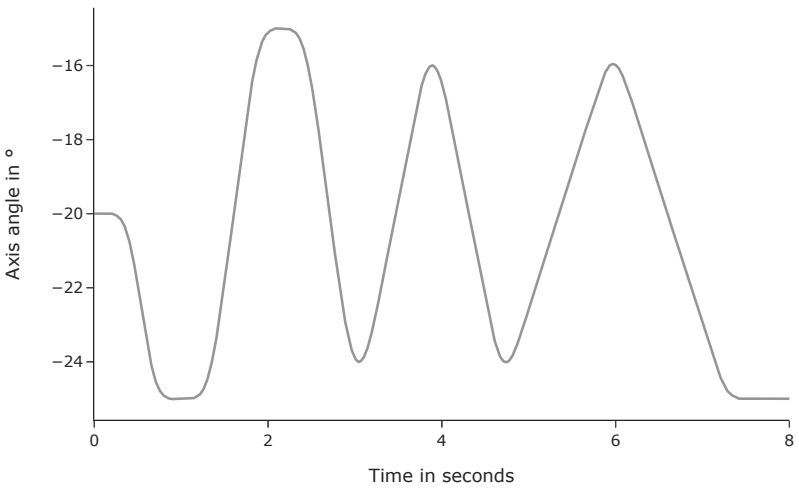

Figure 3. Measurement trajectory for the temperature sensitivity analysis

Preprints (www.preprints.org) | NOT PEER-REVIEWED | Posted: 30 April 2021 doi:10.20944/preprints202104.0797.v1

The second data set was derived from another experiment. Here, the second axis of an ABB IRB 7600-340/2.8 was moved in an angle area of 80° continuously over the time frame of three months. The vibration sensor attached to the gearbox cap of axis 2 sampled with 20 kHz and one measurement lasted 2.15s . The experiment ended after a roller element of a bearing had cracked and had blocked the gear. In this time range 920 vibration measurements were taken in total in equidistant time steps.

3. Results

This section is divided in three parts. First of all, the results from the FEMTO data set analysis are shown. Secondly, the results from the temperature sensitivity analysis are presented. Finally, the application of the HIs on the two accelerated wear tests is described.

3.1. FEMTO data set analysis

From the 16 bearing experiments the HIs presented in table 1 were calculated. We used the first 100 measurements per bearing as the reference quantity for the Z-score-HI and set R to 128. Figure 4 shows the R^2 values for a selection of different HIs as a box plot. The R^2 statistics for all HIs can be found in Appendix A. The abbreviations of the HIs are explained in Table 1. The PtP-, Peak-, RMS-, Std- and Z-score-HI show the highest R^2 values in average. They also show the lowest variance between the different bearings. This means that these HIs detect different faults most reliably. Other HIs show also high trend values but only for some of the bearings. HIs derived from the frequency (DomF, SpC, SpE, SpF, SpRO) domain perform worse compared to HIs from the time domain. The preprocessing steps of enveloping the signal or calculating the residual signal do not affect the HIs trend behaviour significantly, which can be seen in Table A1 - A3.

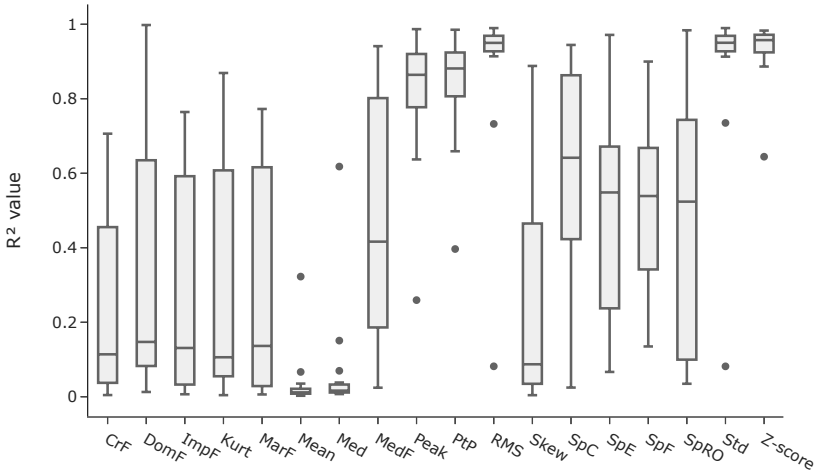

Figure 4. R^2 values for different HIs and bearings from the FEMTO data set based on raw signals

3.2. Temperature sensitivity analysis

Based on this result, we conducted the temperature sensitivity analysis for the PtP-, Peak-, RMS-, Std- and Z-score-HI. Here we used one measurement per temperature step as the reference quantity for the Z-score-HI and set R to 128. Figure 5 shows the change of the HIs per axis in percent. In general, the data from axis 4 show the highest temperature sensitivity for all HIs. The RMS- and Z-score-HI show the lowest temperature sensitivity overall. The comparably higher sensitivty of the HI values derived from data at axis 4

Preprints (www.preprints.org) | NOT PEER-REVIEWED | Posted: 30 April 2021 doi:10.20944/preprints202104.0797.v1

can be related to the robot trajectory. During the trajectory the robot arm was stretched out, which leads to greater elasticitiy at the position of the sensor at axis 4. This can cause increased vibrations, which are magnified under changing temperature influences.

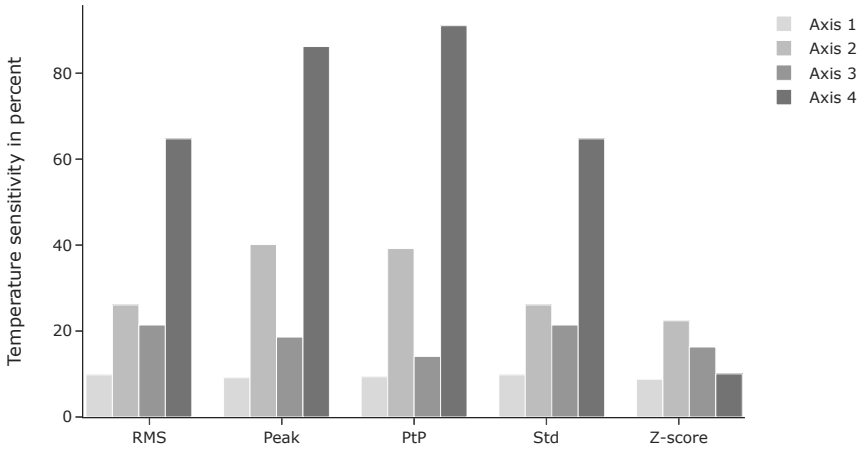

Figure 5. Temperature sensitivity for different HIs and robot axes

3.3. Accelerated wear tests analysis

Given this fact, we analysed the data sets from the accelerated wear tests with only the RMS- and the Z-score-HI. We used the first 100 measurements as the reference quantity for the Z-score-HI and set R to 256. For smoothing, we applied a rolling average with a window length of 15 on both HI series. The progress of the HIs in the accelerated wear test of the ABB IRB 7600 is shown in Figure 6.

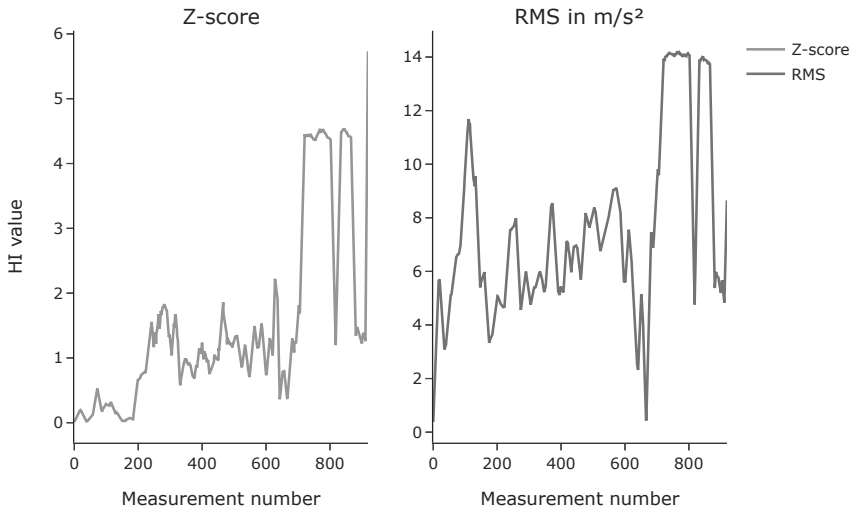

Figure 6. Z-score-HI and RMS-HI for the IRB 7600 experiment

Preprints (www.preprints.org) | NOT PEER-REVIEWED | Posted: 30 April 2021 doi:10.20944/preprints202104.0797.v1

Both HIs show a plateau with increased values at the end of the experiment. It can be assumed that at this point in time faults have already been present. Here, the increased HI values over a longer time period could have been used as a decision criterion for maintenance actions.The measurements at the very end show decreased values again. We assume that this decrease is correlated to a part of the bearing roller. In the end of the experiment, one of the roller elements showed a large pit. During the measurements showing the higher HI values this detached part of the roller element could have been still slightly fixed at the roller element and thus could have caused high vibration. After full detachment, this noise level decreased again. For the measurements before the plateau the RMS-HI shows higher fluctuations compared to the Z-score-HI. For instance, the RMS-HI shows a first high peak around measurement 100. Such peaks could lead to false alarms in a condition monitoring scenario and should be avoided.

The progress of the HIs in the other accelerated wear test performed with the ABB IRB 6600 is shown in Figure 7.

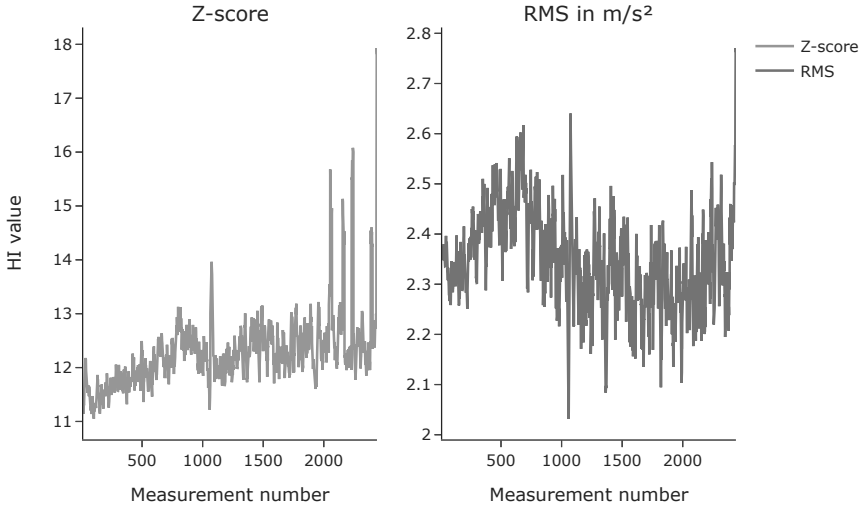

Figure 7. Z-score-HI and RMS-HI for the IRB 6640 experiment

Here, the Z-score-HI shows a trending behaviour, the RMS shows a stationary progress. Both HIs show a high increase during the last measurements. In this experiment, the trending behaviour of the Z-score could have been a criterion to execute maintenance actions. This information is not present in the RMS-progress. Based on the fact that the Z-score showed a better trend behaviour in the ABB IRB 6600 experiment and less noisy behaviour in the ABB IRB 7600 experiment, we suggest the use of the Z-score-HI for the condition monitoring of robot gears.

4. Discussion

The discussion is divided in four parts. First of all, some remarks regarding our designed HI are given. Afterwards, three parts take up one of the Results subsections.

To derive the spectrograms required for the Z-score-HI, the length of the window function must be defined. High values for R result in a high frequency resolution, low values in a high time resolution. For the individual experiments, we chose window lengths that lead to a good compromise between time and frequency resolution by inspecting spectrograms created with different window lengths. We chose window lengths that lead to spectrograms appearing the least noisy in a visual inspection. In an

Preprints (www.preprints.org) | NOT PEER-REVIEWED | Posted: 30 April 2021 doi:10.20944/preprints202104.0797.v1

industry setting, an automated approach should be developed for this dependent on the robot's trajectory and the used sensor.

The motivation to use the FEMTO data set to investigate HI performance was to assess HIs' capability to detect multiple faults. Within a robot gearbox, which are mostly RV reducers, not only bearings but also the gear teeth can have faults. Such faults are not taken into account by our analysis explicitly. However, the bearing faults present in the FEMTO data set, e.g. pitting, are similar to typical gear teeth or shaft damage from a signal analysis point of view. Damage from all components modulate the acceleration signals at a specific frequency and its sidebands. Exactly this capability to track such changes in the signal was investigated in our analysis. There also exist HIs that track energy changes at the specific component fault frequencies. Such HIs were excluded from our analysis because expert knowledge about the geometric characteristics of the gears, e.g., the bearing diameters or the number of roller elements, is required to calculate these HIs. This expert knowledge is usually not available to industrial robot users. We also excluded HIs that could be derived automatically from machine learning models such as autoencoders as the physical interpretation of these HIs is difficult and hence a transferability between different robot systems is questionable from our point of view.

Regarding the results of the temperature sensitivity analysis, it must be pointed out that the results are valid only for the chosen robot trajectory. As the dynamic behaviour of the robot changes within its working space, this analysis should be performed individually for trajectories and robot systems. However, from a theoretical point of view the Z-score-HI possesses the ability to cope with these temperature fluctuations independently of the trajectory. Temperature variations lead to variance in the time-frequency-spectrograms. This variance is taken into account in the $spec(\tau, \omega)_{avg,ref}$ and $spec(\tau, \omega)_{std,ref}$ during the initialisation phase. Hence, Z-score-HIs derived from measurements from functional robot gears and different temperatures will show only little differences in the Z-score-HI value.

Finally, the results from the accelerated wear tests show noisy progress over time. This hinders a simple or automated detection of faults in a condition monitoring behaviour. To establish an automated CM system, a suitable trend detection in combination with an outlier detection system must be set up. A trend detection system could identify HI progress shown as in Figure 7, whereas an outlier detection system could detect progress as depicted in Figure 6. The development of such a system also marks the outlook of our future work.

5. Conclusions

Condition monitoring of robot gears has the potential to decrease production system downtimes. The state-of-the-art provides many health indicators to track the health state of gears. We analysed these health indicators regarding specific requirements rising from typical industrial robot applications. These requirements are the ability to detect different faults, low temperature sensitivity and the capability to deal with instationary velocity behaviour. Additionally, we suggested a new health indicator based on time frequency domain spectrograms and Z-scores that can cope with these requirements. Our analysis showed that the RMS health indicator and our suggested health indicator meet the defined requirements the best. Data from accelerated wear tests shows that for an automatic condition monitoring system a combination of a trend detection and an outlier detection system that can deal with a noisy signal is required.

Author Contributions: Conceptualization, C.N. and G.R.; methodology, C.N.; software, C.N.; validation, C.N.; formal analysis,C.N.; investigation,C.N.; resources, G.R.; data curation, C.N.; writing—original draft preparation, C.N.; writing—review and editing, G.R.; visualization, C.N.; supervision, G.R.; project administration, C.N.; funding acquisition, G.R. All authors have read and agreed to the published version of the manuscript.

 doi:10.20944/preprints202104.0797.v1

Funding: We express our gratitude to the Bavarian Ministry of Economic Affairs, Regional Development and Energy for the funding of our research. The formulated outlook will be investigated as part of the research project "KIVI" (grant number IUK-1809-0008 IUK597/003) and will be further developed and implemented.

Conflicts of Interest: The authors declare no conflict of interest. The funders had no role in the design of the study; in the collection, analyses, or interpretation of data; in the writing of the manuscript, or in the decision to publish the results.

Data Availability Statement: The data presented in this study are available on request from the corresponding author. The data are not publicly available due to confidentiality reasons.

Preprints (www.preprints.org) | NOT PEER-REVIEWED | Posted: 30 April 2021 doi:10.20944/preprints202104.0797.v1

Appendix A

Table A1. R^2 statistics for HIs derived from the normal signal

	CrF	DomF	ImpF	Kurt	MarF	Mean	Med	MedF	Peak	PtP	RMS	Skew	SpC	SpE	SpF	SpRO	Std	Zscore
Mean	0.231	0.354	0.287	0.336	0.296	0.034	0.063	0.467	0.822	0.844	0.887	0.242	0.599	0.488	0.514	0.491	0.887	0.934
Std	0.246	0.351	0.289	0.334	0.298	0.076	0.147	0.311	0.173	0.145	0.215	0.289	0.298	0.281	0.225	0.322	0.215	0.080
Min	0.005	0.013	0.007	0.004	0.006	0.003	0.007	0.024	0.259	0.397	0.082	0.004	0.025	0.067	0.135	0.035	0.082	0.644
Max	0.706	0.998	0.764	0.869	0.773	0.323	0.618	0.941	0.987	0.985	0.990	0.888	0.944	0.971	0.900	0.984	0.990	0.983

Table A2. R^2 statistics for HIs derived from the enveloped signal

	CrF	DomF	ImpF	Kurt	MarF	Mean	Med	MedF	Peak	PtP	RMS	Skew	SpC	SpE	SpF	SpRO	Std
Mean	0.215	0.139	0.284	0.299	0.296	0.776	0.819	0.496	0.816	0.816	0.872	0.275	0.605	0.464	0.462	0.514	0.898
Std	0.229	0.248	0.283	0.328	0.291	0.296	0.248	0.318	0.178	0.178	0.227	0.303	0.286	0.298	0.276	0.309	0.131
Min	0.005	0.001	0.006	0.001	0.005	0.010	0.014	0.023	0.246	0.246	0.074	0.008	0.046	0.013	0.012	0.007	0.427
Max	0.635	0.997	0.741	0.919	0.766	0.977	0.983	0.981	0.988	0.988	0.989	0.905	0.939	0.978	0.901	0.987	0.987

Table A3. R^2 statistics for HIs derived from the residual signal as suggestet by [4]

	CrF	DomF	ImpF	Kurt	MarF	Mean	Med	MedF	Peak	PtP	RMS	Skew	SpC	SpF	SpRO	Std	SpE
Mean	0.329	0.423	0.348	0.365	0.355	0.032	0.088	0.608	0.847	0.859	0.884	0.237	0.701	0.609	0.605	0.884	0.534
Std	0.270	0.348	0.303	0.337	0.312	0.089	0.187	0.292	0.178	0.153	0.221	0.319	0.196	0.202	0.213	0.221	0.316
Min	0.010	0.021	0.003	0.007	0.018	0.001	0.001	0.016	0.211	0.328	0.082	0.003	0.425	0.147	0.132	0.083	0.023
Max	0.802	0.992	0.828	0.858	0.830	0.374	0.671	0.988	0.987	0.987	0.990	0.943	0.959	0.930	0.977	0.990	0.969

References

1. Krockenberger, O. Industrial Robots for the Automotive Industry. *SAE Technical Paper Series* **1996**. doi:10.4271/962393.
2. Lee, J.; Wu, F.; Zhao, W.; Ghaffari, M.; Liao, L.; Siegel, D. Prognostics and health management design for rotary machinery systems–Reviews, methodology and applications. *Mechanical Systems and Signal Processing* **2014**, *42*, 314–334. doi:10.1016/j.ymssp.2013.06.004.
3. ISO. *DIN ISO 17359:2018-05, Zustandsüberwachung und -diagnostik von Maschinen - Allgemeine Anleitungen (ISO_17359:2018)*; Beuth Verlag GmbH: Berlin, 2018. doi:10.31030/2838751.
4. Kim, Y.; Park, J.; Na, K.; Yuan, H.; Youn, B.D.; Kang, C.s. Phase-based time domain averaging (PTDA) for fault detection of a gearbox in an industrial robot using vibration signals. *Mechanical Systems and Signal Processing* **2020**, *138*, 106544. doi:10.1016/j.ymssp.2019.106544.
5. Jaber, A.A. *Design of an Intelligent Embedded System for Condition Monitoring of an Industrial Robot*; Springer Theses, Recognizing Outstanding Ph.D. Research, Springer International Publishing: Cham and s.l., 2017. doi:10.1007/978-3-319-44932-6.
6. Zhi, H.; Yangi-Shang. Remote performance evaluation, life prediction and fault diagnosis of RV reducer for industrial robot. *Journal of Physics: Conference Series* **2020**, *1676*, 012212. doi:10.1088/1742-6596/1676/1/012212.
7. Danielson Hugo.; Schmuck Benjamin. Robot Condition Monitoring: A first step in Condition Monitoring for robotic applications. Master's thesis, Lulea University of Technology, Lulea, 2017.
8. Martin Karlsson.; Fredrik Hörnqvist. Robot Condition Monitoring and Production Simulation. Master's thesis, Lulea University of Technology, Lulea, 2018.
9. Liu, X.; Wu, X.; Liu, C.; Liu, T. Research on condition monitoring of speed reducer of industrial robot with acoustic emission. *Transactions of the Canadian Society for Mechanical Engineering* **2016**, *40*, 1041–1049. doi:10.1139/tcsme-2016-0086.
10. Sun, H.; Zhang, J. Health Monitoring of Strain Wave Gear on Industrial Robots.
11. Larsen, R.J.; Marx, M.L. *An introduction to mathematical statistics and its applications*, 3. ed. ed.; Prentice Hall: Upper Saddle River NJ i.a., 2001.
12. Nectoux, P.; Gouriveau, R.; Medjaher, K.; Ramasso, E.; Chebel-Morello, B.; Zerhouni, N.; Varnier, C. PRONOSTIA : An experimental platform for bearings accelerated degradation tests. IEEE International Conference on Prognostics and Health Management, PHM'12.; ; Vol. sur CD ROM.
13. Arun, P.; Lincon, S.A.; Prabhakaran, N. Detection and Characterization of Bearing Faults from the Frequency Domain Features of Vibration. *IETE Journal of Research* **2018**, *64*, 634–647. doi:10.1080/03772063.2017.1369369.
14. Caesarendra, W.; Tjahjowidodo, T. A Review of Feature Extraction Methods in Vibration-Based Condition Monitoring and Its Application for Degradation Trend Estimation of Low-Speed Slew Bearing. *Machines* **2017**, *5*, 21. doi:10.3390/machines5040021.
15. Vecer, P.; Kreidl, M.; Smid, R. Condition Indicators for Gearbox Condition Monitoring Systems. *Acta Polytechnica* **2005**, *45*, 35–42.
16. Zhu, J.; Nostrand, T.; Spiegel, C.; Morton, B. Survey of condition indicators for condition monitoring systems **2014**.
17. Geropp, B. Envelope Analysis - A Signal Analysis Technique for Early Detection and Isolation of Machine Faults. *IFAC Proceedings Volumes* **1997**, *30*, 977–981. doi:10.1016/S1474-6670(17)42527-4.